

SUPPORTING INFORMATION

***N,N*-Ru(II)-*p*-cymene-poly(*N*-vinylpyrrolidone) Surface Functionalized Gold Nanoparticles: From Organoruthenium Complex to Nanomaterial for Antiproliferative Activity**

Durairaj Gopalakrishnan,^a S. Saravanan,^a Ronald Merckx,^b Arumugam Madan Kumar,^c Themmila Khamrang,^d Marappan Velusamy,^e K. Vasanth,^f S. Sunitha,^c Richard Hoogenboom,^b Samarendra Maji*^a and Mani Ganeshpandian*^a

^aDepartment of Chemistry, SRM Institute of Science and Technology, Kattankulathur 603203, Chengalpattu, Chennai, TN, India.

^bSupramolecular Chemistry Group, Centre of Macromolecular Chemistry (CMaC), Department of Organic and Macromolecular Chemistry, Ghent University, Krijgslaan 281 S4, Ghent, Belgium

^cDepartment of Chemistry, Sathyabama Institute of Science and Technology, Chennai – 600119, India.

^dDepartment of Chemistry, C. I. College, Bishnupur 795126, Manipur, India

^eDepartment of Chemistry, North Eastern Hill University, Shillong 793022, India

^fDivision of Molecular biology, Interdisciplinary Institute of Indian System of Medicine (IIISM), SRM Institute of Science and Technology, Kattankulathur 603 203, Kanchipuram, Chennai, TN, India.

*Email: samarenr@srmist.edu.in (S.M); ganeshpm@srmist.edu.in (M. G)

EXPERIMENTAL SECTION

Materials.

The reagents and chemicals were purchased from commercial sources (Sigma-Aldrich, USA; Himedia, India; Merck, India; SRL, India). $[(\eta^6\text{-}p\text{-cymene})\text{RuCl}_2]_2$ precursor, $[(\eta^6\text{-benzene})\text{RuCl}_2]_2$ precursor, acenaphthenequinone, anhydrous ZnCl_2 , *p*-anisidine, anhydrous K_2CO_3 , $\text{HAuCl}_4\cdot 3\text{H}_2\text{O}$, sodium citrate, pBR322 supercoiled DNA were used as delivered. *N*-vinylpyrrolidone (NVP, 99%, Acros) was purified by vacuum distillation. AIBN was recrystallized twice from methanol before use. HPLC grade solvents *N,N*-dimethylacetamide (DMA), dichloromethane and diethyl ether were obtained from Sigma Aldrich, *N,N*-

dimethylformamide (DMF) from Biosolve, and *n*-hexane from Fischer Scientific. Ultrapure Millipore-filtered water was used in all experiments. Tris(hydroxymethyl) aminomethane·HCl (Tris-HCl) (pH 7.1) was prepared by the reported procedure.¹ Bis(4-methoxyphenylimino)acenaphthene (bman) ligand was synthesized by using reported procedure.²

Characterizations.

Microanalysis (C, H, and N) were carried out with a Vario EL elemental analyzer. UV-Vis spectroscopy was recorded on a Specord 210 UV-Vis spectrophotometer using cuvettes of 1 cm path length. ¹H NMR spectra were recorded on a Bruker 300 and 500 MHz NMR spectrometer. Mass spectrometry was performed on a Shimadzu LC MS-2020 spectrometer. Gas chromatography was performed on a 7890A from Agilent Technologies with an Agilent J&W Advanced Capillary GC column (30 m, 0.320 mm, and 0.25 mm). Injections were performed with an Agilent Technologies 7693 autosampler. Detection was done with a FID detector. Injector and detector temperatures were kept constant at 250 and 280 °C, respectively. The column was initially set at 50 °C, followed by two heating stages: from 50 °C to 120 °C with a rate of 20 °C/min and from 100 °C to 300 °C with a rate of 50 °C/min, and then held at this temperature for 0.5 minutes. Conversions of the monomers were determined based on the integration of monomer peaks using the polymerization solvent, anisole, as an internal standard. Size-exclusion chromatography (SEC) was performed on a Agilent 1260-series HPLC system equipped with a 1260 online degasser, a 1260 ISO-pump, a 1260 automatic liquid sampler (ALS), a thermostatted column compartment (TCC) at 50°C equipped with two PLgel 5 μm mixed-D columns and a precolumn in series, a 1260 diode array detector (DAD) and a 1260 refractive index detector (RID) to determine the molecular weights and molecular weight distributions of the polymers. The used eluent was DMAc containing 50 mM of LiCl at a flow rate of 0.500 mL/min. The spectra were analyzed using the Agilent Chemstation software with the GPC add-on. Molar mass values and Đ values were calculated against PMMA standards from PSS. Matrix-assisted laser desorption/ionization time-of-flight mass spectrometry (MALDI-TOF MS) was performed on an Applied Biosystems/MDS SCIEX 4800 MALDI TOF/TOFTM Analyzer, which is the next generation of tandem time-of-flight MS/MS systems. The 4800 MALDI TOF/TOFTM Analyzer uses a diode-pumped, solid-state laser. Under normal operating conditions, the instrument is categorized as a Class 1 laser. Mass spectra were obtained with an accelerating

potential of 20 kV in positive ion mode and either reflection or linear mode. Trans-2-[3-(4-*tert*-butylphenyl)-2-methyl-2-propenylidene]malononitrile (DCTB, 98%, TCI, 20 mg/mL in acetone) was used as matrix. Polymer samples were dissolved in acetone or methanol (2 mg/mL) and applied on the sample plate via the dried droplet method (0.5 μ L) in between 0.5 μ L of matrix solutions. A poly(ethylene oxide) standard ($M_n = 2000$ g/mol) was used for calibration. All data were processed using the Data Explorer 4.0.0.0 (Applied Biosystems) software package. Transmission electron microscope (TEM) images were collected from HR-TEM (JEM-2100 Plus Electron Microscope, Japan). Particle size distribution and zeta potential measurements were recorded on zetasizer 90 (Malvern Panalytical, UK). Supercoiled plasmid pBR322 DNA was stored at -20 $^{\circ}$ C.

Synthesis of [Ru(η^6 -*p*-cymene)(bman)Cl]PF₆ (Ru(*p*-cym)(NN)(Cl))

To a suspension of ruthenium dimer precursor [$(\eta^6$ -*p*-cymene)RuCl₂]₂ (0.41 g, 0.654 mmol) in methanol (25 ml), bman ligand (0.52 g, 1.308 mmol) was added. The mixture was stirred at 40 $^{\circ}$ C for 6 h under N₂ atmosphere and the resulting brownish solution was filtered. The solvent was reduced into small volume (5 ml) and then NH₄PF₆ (0.25 g, 1.5 mmol) was added to get a complex [Ru(η^6 -*p*-cymene)(bman)Cl]PF₆ as a brownish solid. The product obtained was washed with small amount of cold methanol and excess of diethyl ether and dried in vacuum. Yield: 81%. Suitable crystals for X-ray diffraction studies were obtained from acetonitrile/dichloromethane mixture (10:1 v/v) solution of complex. ESI-MS, ¹H NMR and crystal structure are shown in **Figures S1, S2 and (S3 and S4)** respectively. Anal. calcd for [Ru(η^6 -*p*-cymene)(bman)Cl]PF₆: C, 53.50; H, 4.24; N, 3.47. Found: C, 53.46; H, 4.38; N, 3.36 %. ESI-MS: [Ru(η^6 -*p*-cymene)(bman)Cl]⁺ displays a peak at *m/z* 662.60 (calcd 663.14). ¹H NMR (500 MHz, DMSO-*d*₆): δ 1.11 (s, 6H, CH(CH₃)₂), 2.13 (s, 3H, CH₃, *p*-cymene), 2.60 (m, 1H, CH(CH₃)₂), 3.95 (s, 6H, OCH₃), 5.37-5.41 (dd, 4H, η^6 -C₆H₄), 7.14-8.29 (14H, aromatic, bman) ppm. ¹³C NMR (125 MHz, DMSO-*d*₆): δ 172.64, 159.85, 143.91, 142.96, 131.98, 130.87, 128.80, 124.97, 124.09, 108.42, 102.67, 87.19, 86.51, 55.65, 39.85, 39.69, 39.35, 39.19, 30.50, 21.58, 18.18. UV-Vis. (c, 120 μ M; CH₃CN; λ_{\max} nm, (ϵ M⁻¹ cm⁻¹): 252 (20,132), 451 (3267).

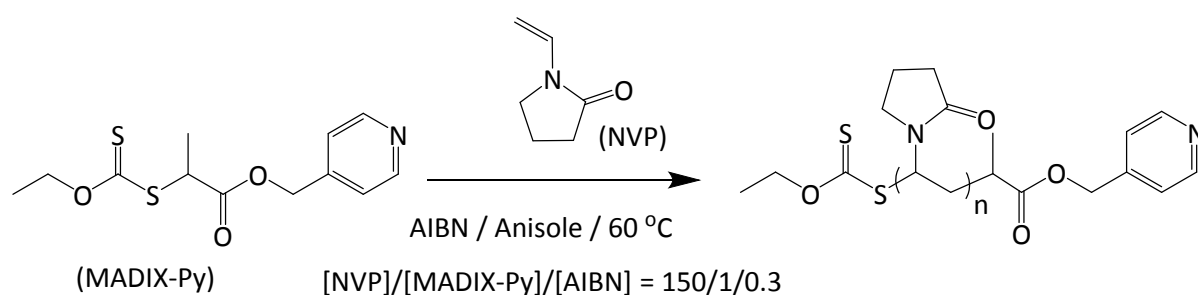
Synthesis of MADIX-Py CTA

RAFT/MADIX CTA (MADIX-Py) was synthesized by two steps. At first xanthate CTA, 2-((ethoxycarbonothioyl)thio)propanoic acid was synthesized by a general procedure described previously by Klumperman et al.³ Potassium O-ethyl xanthate (9.96 g, 0.0621 mol) was dissolved in 30 mL of distilled water. Then 15 mL of 3.3 M NaOH was added while stirring in an ice bath. Later, 2-bromopropionic acid (7.6 g, 0.0497 mol) was added dropwise with stirring. The reaction was continued for 16 h at room temperature. The pH of the solution was adjusted to pH 1 with 2 M HCl. The product was extracted with diethyl ether (2 x 200 mL), the organic phase was dried over anhydrous MgSO₄ and the solvent was evaporated under reduced pressure to obtain a pale yellow liquid. Finally the crude product was recrystallized from hexane. (Yield: 75%). ¹H NMR spectrum of the ECTTPA is shown in **Figure S5**. In the next step, ECTTPA (1.96 g, 10.08 mmol), Py-OH (1.0 g, 9.16 mmol) and DMAP (123 mg, 1.0 mmol) were introduced into a round-bottom flask and dissolved in anhydrous dichloromethane (DCM, 55 mL). The reaction mixture was cooled to 0°C in an ice bath and a solution of EDC (2.13 g, 11.08 mmol) in DCM (10 mL) was added drop-wise while vigorously stirring.⁴ The reaction mixture was stirred in an ice bath for 2h and subsequently at room temperature overnight. The solvent was evaporated under vacuum. The crude product was purified by column chromatography on silica gel using dichloromethane (DCM) and ethyl acetate as eluent. The second fraction was collected and the solvent was removed under reduced pressure to obtain the product as yellow liquid (2.523 g, yield: 88%). (Note: by storing for longer time it changes its colour from yellow to dark brown). ¹H NMR spectrum of the MADIX-Py CTA is shown in **Figure S6**. LC-MS of MADIX-Py CTA is shown in **Figure S7**.

Synthesis of PNVP

The MADIX/RAFT polymerization of NVP was performed in a 25 mL Schlenk tube under argon atmosphere.⁵ NVP (2 g, 18.0 mmol), freshly prepared MADIX-Py (34.24 mg, 0.12 mmol), AIBN (5.91 mg, 3.6 x 10⁻² mmol) and 4 mL anisole were added to the Schlenk tube at a molar ratio of monomer/CTA/AIBN of 150/1/0.3. The Schlenk tube containing the reaction mixture was degassed by bubbling argon (Ar) through the solution for 40 min keeping on ice cold water the Schenk flask was placed in an oil bath set at 60 °C for 2.5 h. The polymer was isolated by precipitation in hexane/DEE (9:1). Further, the polymer was dissolved in dichloromethane (DCM) and re-precipitated in hexane three times and were recovered as a

white powder after centrifugation. By determining the monomer conversion via gas chromatography (GC), a theoretical molecular weight, $M_{n,th}$, of 2800 g/mol was measured. ^1H NMR spectrum of the purified polymer is shown in **Figure S8**. Molecular weight of the polymer via end group analysis was found to be 3400 g/mol. Size exclusion chromatography (SEC) measured in dimethylacetamide (DMA) against PMMA standards is shown in **Figure S9**. Molecular weight of the polymer could not determine as the polymer peak appear outside the PMMA calibration range. A MALDI-TOF mass spectrometry analysis was performed on this PNVP sample after purification (**Figure S10**).



Scheme S1. Reaction scheme for the MADIX/RAFT homo-polymerization of NVP using MADIX-Py as chain transfer agent (CTA).

Synthesis of $[\text{Ru}(p\text{-cym})(\text{NN})(\text{PNVP-Py})]\text{Cl}_2$ ($\text{Ru}(p\text{-cym})(\text{NN})(\text{PNVP-Py})$)

The $[\text{Ru}(p\text{-cym})(\text{NN})\text{Cl}]\text{PF}_6$ complex (0.40 g, 0.5 mmol) and equivalent amount of AgNO_3 (0.085 g, 0.5 mmol) in 1:1 mixture of methanol/ H_2O (20 ml) solvent were taken in aluminium foil-covered RB flask. The mixture was refluxed for 6 h and then the solution was filtered to remove AgCl . Later, 20-fold excess of the PNVP-Py in water was added to the mixture and stirred for 48 h under N_2 atmosphere. The colour of the solution was changed from brownish yellow to dark green. To this solution, an excess equivalent of NH_4PF_6 (0.10 g, 0.65 mmol) was added and the resulting mixture was stirred for 2 h to get the precipitate of $\text{Ru}(p\text{-cym})(\text{NN})(\text{PNVP-Py})$ as a PF_6 salt. The $\text{Ru}(p\text{-cym})(\text{NN})(\text{PNVP-Py})(\text{PF}_6)_2$ was recovered by centrifugation and washed with water to remove excess PF_6 anions. To get the $\text{Ru}(p\text{-cym})(\text{NN})(\text{PNVP-Py})$ in aqueous solution, the PF_6 solid was re-dispersed in acetonitrile and concentrated solution of tetrabutylammonium chloride was added and the resulting mixture was stirred for 2 h. The flocculate that formed was collected by centrifugation and washed with acetone and dried under high vacuum resulting the formation of $[\text{Ru}(p\text{-$

cym)(NN)(PNVP-Py)]Cl₂. The concentration of metallopolymer was calculated according to the extinction coefficient of the MLCT band of complex.

Synthesis of Ru(*p*-cym)(NN)(PNVP-Py)@AuNPs

Synthesis of AuNPs and functionalisation of AuNPs using Ru(*p*-cym)(NN)(PNVP-Py) was achieved by adopting the method reported by Gunnlaugsson *et al* in literature.⁶ HAuCl₄·3H₂O (0.040 g) was taken clean conical flask and dissolved in 100 ml Millipore water. The flask was heated on hot plate while stirring. When the solution starts to reflux, 38.8 mM aqueous solution of sodium citrate was quickly added resulting the colour change of solution from pale yellow to ruby red in 1 min. The solution was allowed to reflux further 10 minutes and then left to cool down at room temperature. For the functionalization of the AuNPs with the Ru(II)-metallopolymer, 1.5 mL of a 0.7 × 10⁻³ M aqueous solution of Ru(*p*-cym)(NN)(PNVP-Py) was added into 3 mL of the AuNPs solution (3.38 × 10⁻⁴ M) in water. The mixture was left stirring for 12 h and then concentrated aqueous solution of NH₄PF₆ (0.5 mL) was afforded flocculation of a dark solid which was collected by centrifugation and washed with H₂O (3 × 10 mL). The solid was redissolved in acetonitrile (10 mL) before addition of a conc. solution of tetrabutylammonium chloride to get a flocculate. The flocculate was collected by centrifugation and washed with acetonitrile (3 × 10 mL) before being dried under high vacuum. The concentration of nanocomposite was calculated according to the extinction coefficient of the SPR band of AuNP.

DNA cleavage Studies

The DNA cleavage study was carried out by using agarose gel electrophoresis technique. The super coiled pBR322 plasmid DNA (40 μM) was treated with desired concentration of complexes in 5 mM Tris-HCl/50 mM NaCl buffer at pH 7.1. The samples were incubated for 1h at 37 °C and then a loading buffer containing 25% bromophenol blue, 0.25% xylene cyanol and 30% glycerol (3 μL) was added and electrophoresis was performed at 60 V for 3 h in Tris-Acetate-EDTA (TAE) buffer (40 mM Tris-base, 20 mM, acetic acid, 1 mM EDTA) using 1% agarose gel containing 1.0 μg/mL ethidium bromide. The gels were viewed in a GELSTAN 1312 gel documentation system and photographed using a CCD camera.

X-Ray crystallographic analysis

Single crystals suitable for X-ray diffraction were obtained by slow diffusion of hexane in to a solution of the complex in dichloromethane. The data collection was fulfilled using an

Oxford Diffraction Xcalibur (Eos Gemini) diffractometer at ambient temperature with graphite-monochromated Mo-K α radiation ($\lambda = 0.71073 \text{ \AA}$). Data reduction and processing were carried out using the CrysAlisPro (Agilent Technologies Ltd, Yarnton, UK) suite of programmes. The structure was solved by direct methods and subsequently refined by full-matrix least squares calculations with the SHELEXL-2014 software package. All non-hydrogen atoms were refined anisotropically while hydrogen atoms were placed in geometrically idealized positions and constrained to ride on their parent atoms. The graphics interface package used was PLATON, and the figures were generated using the ORTEP 3.07 generation package.

Cell culture

The human hepatocarcinoma (HepG2), human colorectal adenocarcinoma (HT-29) and non-cancerous human embryonic kidney (HEK293) cell lines were procured from National Centre for Cell Science (NCCS), Pune and maintained in DMEM medium supplemented with 10% FBS containing 100 U/mL penicillin, and 100 $\mu\text{g/mL}$ streptomycin. Cells were grown in T25 flasks at 37°C in a humidified atmosphere containing 5% CO₂. The cells were split every 2–3 days to maintain exponential growth. The cell number was assessed by the standard procedure of cell counting using a hemocytometer.

MTT assay

The Antiproliferative activity was assessed by adopting (3-(4,5-dimethylthiazol-2-yl)2,5-diphenyltetrazolium bromide) (MTT) assay based on the previous report.⁷ Briefly, HT-29, HepG2 and HEK293 cell lines (5×10^3) were seeded in 96-well plates and cultured for 24 h, followed by incubation of compounds with various concentration (2-200 μM) for 24 h. The stock solutions of the compounds were prepared in 5% DMSO/10 mM PBS mixture immediately prior to dilution. Different concentrations of solution were prepared by the dilution of the stock solution using culture media without delay. The solutions were added in triplicate at the appropriate concentrations in the respective wells. The final DMSO concentration in the wells did not exceed 0.2% and the same amount of DMSO was maintained in all the cellular experiments. Therefore, all the experiments were done at non-toxic concentrations of DMSO. Cells treated with 20 μM quercetin for 24 h were considered as a positive control, while the untreated cells incubated with 0.2% DMSO for 24 h at 37 °C were considered as a negative control. After treatment period, the medium was removed and

20 μ L of MTT (5 mg/mL) was added to the cells and incubated at 37 °C for 4 h. The MTT insoluble formazan was dissolved in DMSO and the MTT reduction was quantified by measuring the absorbance at 570 nm (Multiskan Spectrophotometer, USA). The obtained data were plotted and fitted using GraphPad Prism software to calculate the 50% viability (IC_{50}) value. The data were obtained for three biological replicates each and used to calculate the mean. The IC_{50} values provided are mean \pm standard deviation. The statistical significance (*p*-value) of the data, which was determined using GraphPad prism software with t-test, is > 0.002 to < 0.05 . Prior to the experiment, the stability of compounds in 5% DMSO/10 mM PBS was monitored by recording the UV-Vis absorption spectra over 24 h.

AO/EB staining assay

AO/ EB staining was used to evaluate cell and nuclear morphology as described by the previous method.^{8,9} HT-29 (Human Colorectal Adenocarcinoma Cell Line) and HepG2 (Human Liver cancer) cell line for 24 h was seeded on 24 well plate with 10% of FBS medium, around 50,000 cells in each well. Apoptotic assay was performed after treatment with complex and nanoconjugate for 24 h. Three stages of apoptosis was determined through AO/EB staining. AO is a nuclei stain, it will stain both live and dead cells, and EB will penetrate stain the dead cells. 10 μ g/mL of both AO/EB was processed with 5 min incubation. Coverslips were taken, kept on glass slides and stained with 100 μ L of the dye mixture (1:1 ratio of AO and EB), and it was immediately viewed under an inverted fluorescence microscope (EVOS FL digital inverted fluorescence microscope (AMG)). Result were recorded with the Green, yellow, orange and red fluorescent emitting cells based on the live, early apoptosis, late apoptosis and necrosis cells respectively.

Annexin V/PI double staining assay

Apoptosis mediated cell death of human colorectal adenocarcinoma (HT-29) were examined using FITC-labeled Annexin V/PI according to the manufacturer's protocol. HT-29 cells ($1-2 \times 10^5$ cells/well) were incubated at 37°C with 5% CO₂ for 24 h in the presence or absence of compounds at their IC_{50} concentration. After incubation, the cells were trypsinized, washed twice with HBSS, re-suspended in 100 μ L Annexin V binding buffer and then incubated for 20 min, in 5 μ L of Annexin V FITC. 1 μ L of 1 mg/mL PI solution was added to each cell suspension and were run immediately in flow cytometer (FACS Calibur, Becton Dickinson, USA) and analyzed in CellQuest software.

Immunostaining

The control and treated HT-29 cells were fixed with paraformaldehyde followed by permeabilization with 0.25% tris-100 in PBS for 15 min and blocked with 5% bovine serum albumin in PBS. After blocking, the cover slips were incubated with anti-cyclin D1 (1:100) at 4°C overnight and then incubated with Alexa Fluor® 488 secondary antibody (1:1000) was applied for additional 2h at room temperature. Cells were then mounted with DAPI and observed using a LSM 700 confocal microscope (magnification, ×40; Zeiss, Germany) and visualized using ZEN 2012 software.

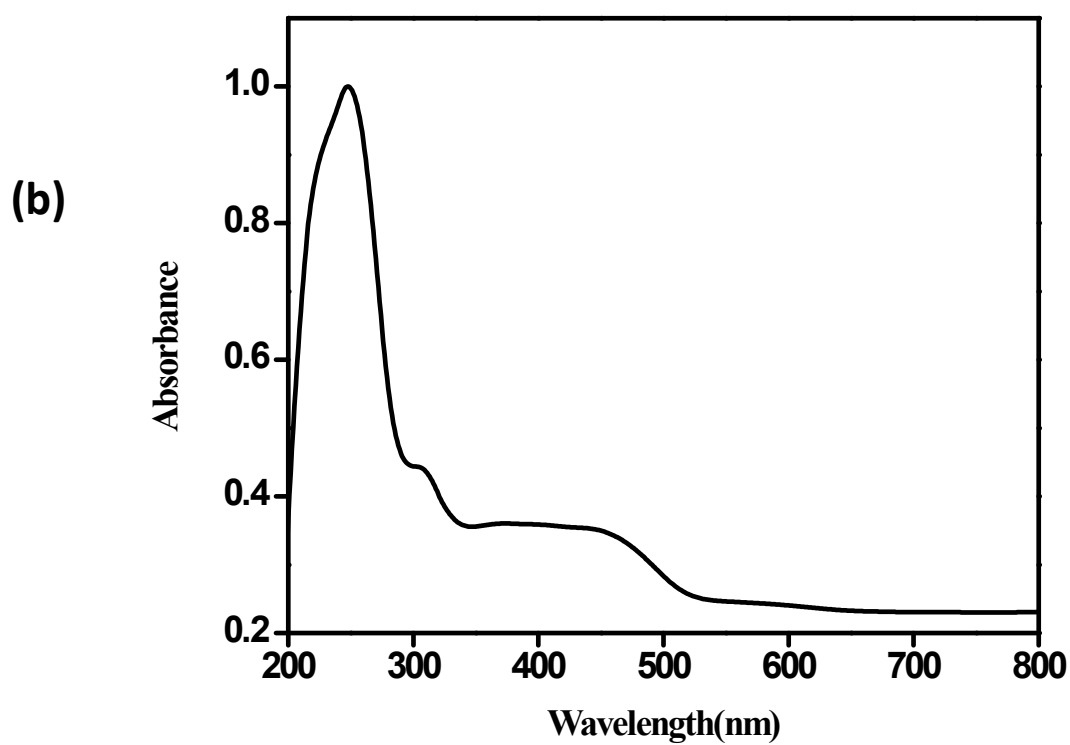
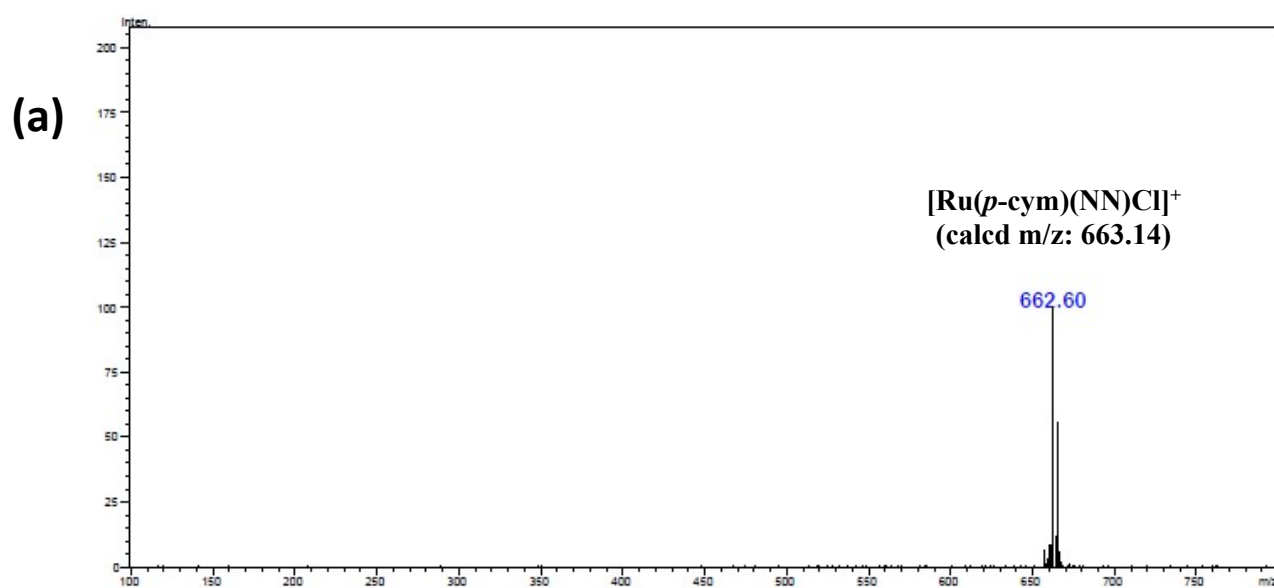


Figure S1. (a) ESI-Mass spectrum of Ru(*p*-cym)(NN)(Cl) in acetonitrile. (b) UV-Vis absorption spectra of Ru(*p*-cym)(NN)(Cl) in acetonitrile.

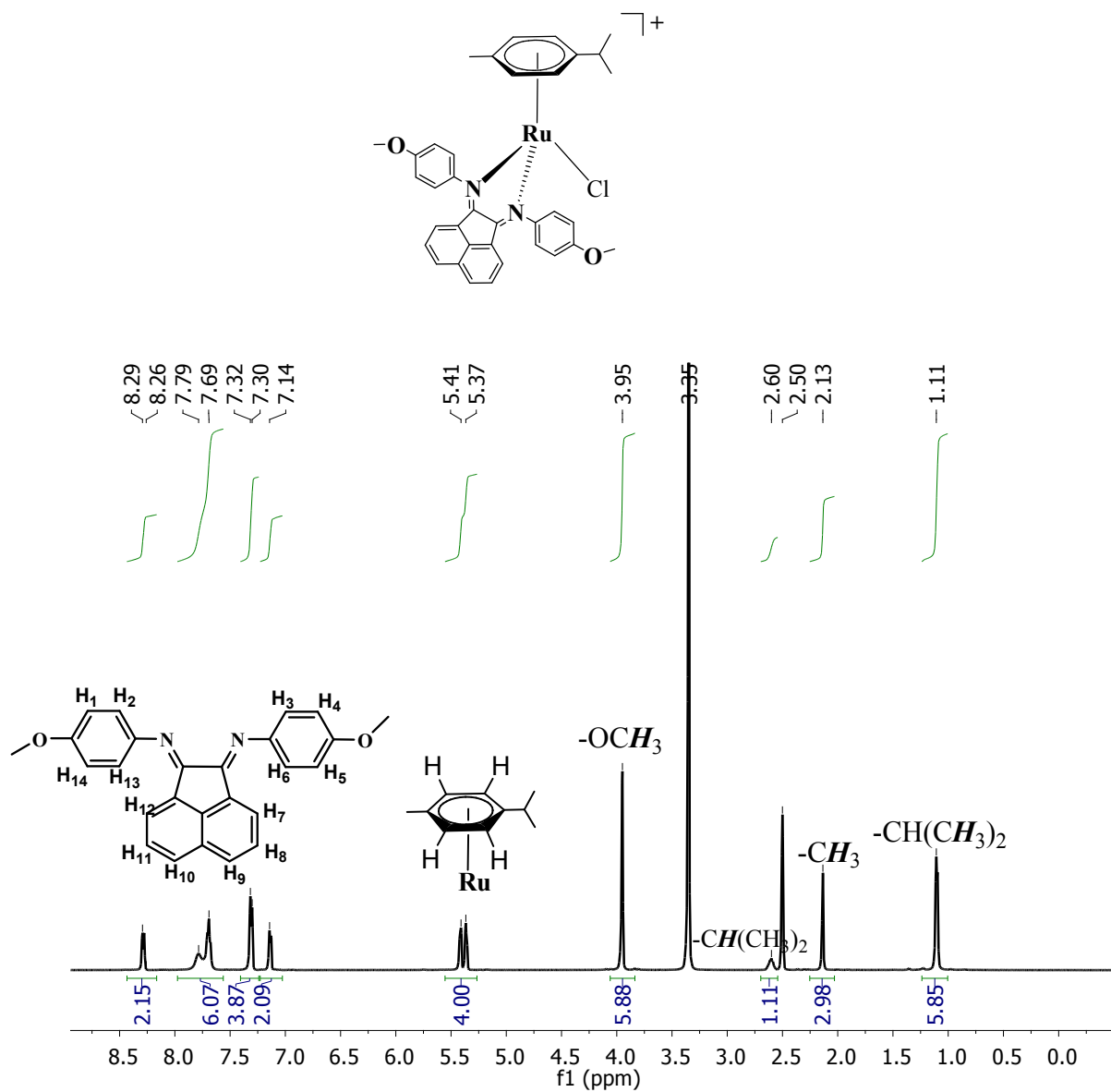


Figure S2. ^1H NMR spectrum of $\text{Ru}(p\text{-cym})(\text{NN})(\text{Cl})$ in $\text{DMSO-}d_6$.

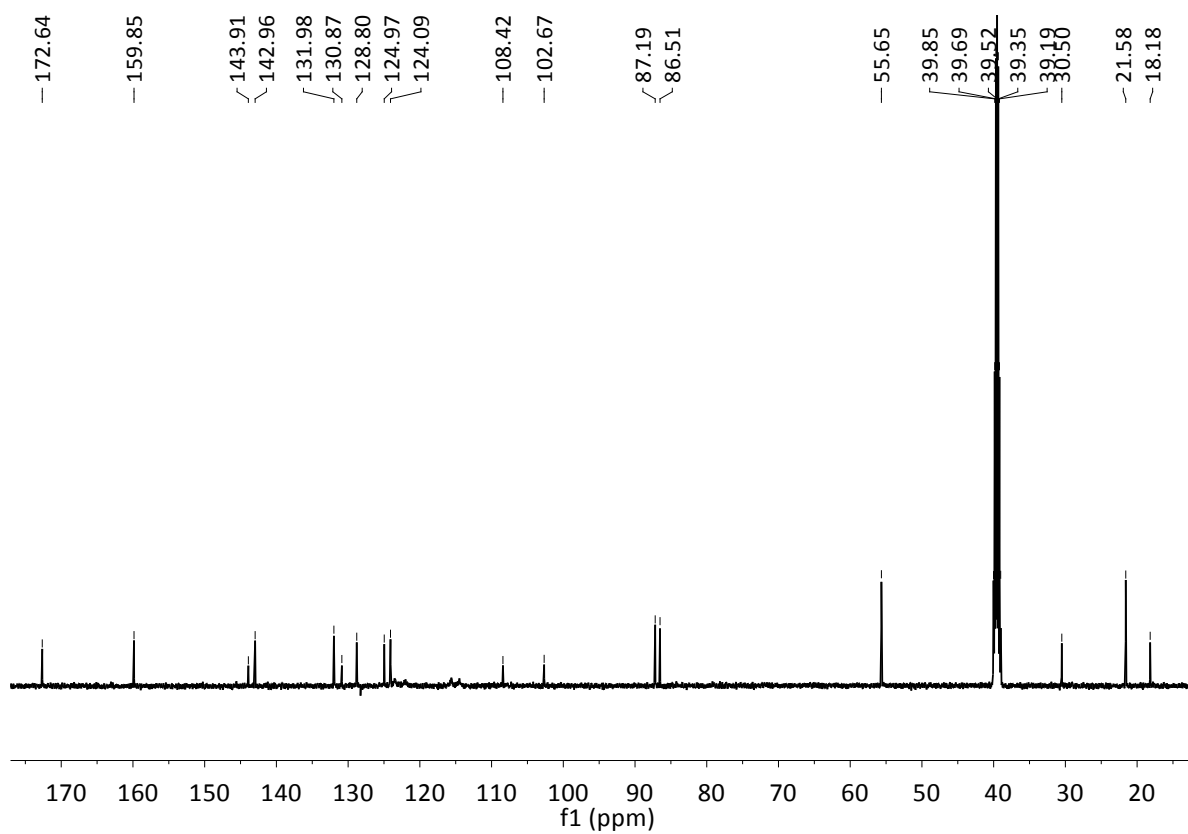


Figure S3. ^{13}C -NMR spectrum of $\text{Ru}(p\text{-cym})(\text{NN})(\text{Cl})$ in $\text{DMSO-}d_6$.

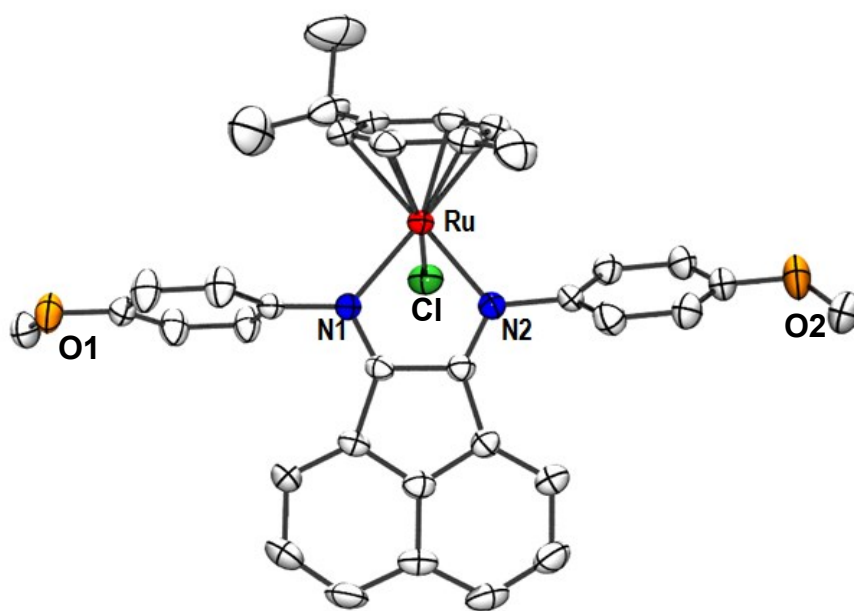


Figure S4. Perspective view of the crystal structure of Ru(*p*-cym)(NN)(Cl). Ellipsoids are drawn at 50% probability level. Hydrogen atoms, PF₆ anion and solvent molecule (CH₂Cl₂) are omitted for the sake of clarity.

Table S1. Crystal data, data collection and structure refinement details for Ru(*p*-cym)(NN)(Cl) complex.

Empirical formula	C ₃₇ H ₃₆ Cl ₃ F ₆ N ₂ O ₂ PRu
Formula weight	893.07
Temperature (K)	293(2)
Wavelength (Å)	0.71073
Crystal system	monoclinic
Space group	P 21/c
a(Å)	10.4890(7)
b(Å)	16.8744(10)
c(Å)	21.4270(12)
α(°)	90
β(°)	97.107(7)
ν(°)	90
Volume (Å ³)	3763.3(4)
Z	4
D _c (g.cm ⁻³)	1.576
μ (mm ⁻¹)	0.738
F(000)	1808
Goodness-of-fit on F ²	1.053
Final R indices [I>2σ (I)]	R ₁ = 0.0665, wR ₂ = 0.1662
R indices (all data)	R ₁ = 0.0861, wR ₂ = 0.1800

Table S2. Selected bond lengths [Å] and bond angles [deg] for Ru(*p*-cym)(NN)(Cl) complex.

Bond length [Å]

Ru(1)-N(1)	2.086(4)
Ru(1)-N(2)	2.078(4)
Ru(1)-Cl(1)	2.384(4)
Ru1-C34	2.186(5)
Ru1-C31	2.191(5)
Ru1-C35	2.205(5)
Ru1-C32	2.205(5)
Ru1-C33	2.209(5)
Ru1-C30	2.225(5)
Ru-C _{ave}	2.203(5)

Bond angle [deg]

N(1)-Ru(1)-N(2)	77.53(16)
N(1)-Ru(1)-Cl(1)	84.67(12)
N(2)-Ru(1)-Cl(1)	83.58(11)

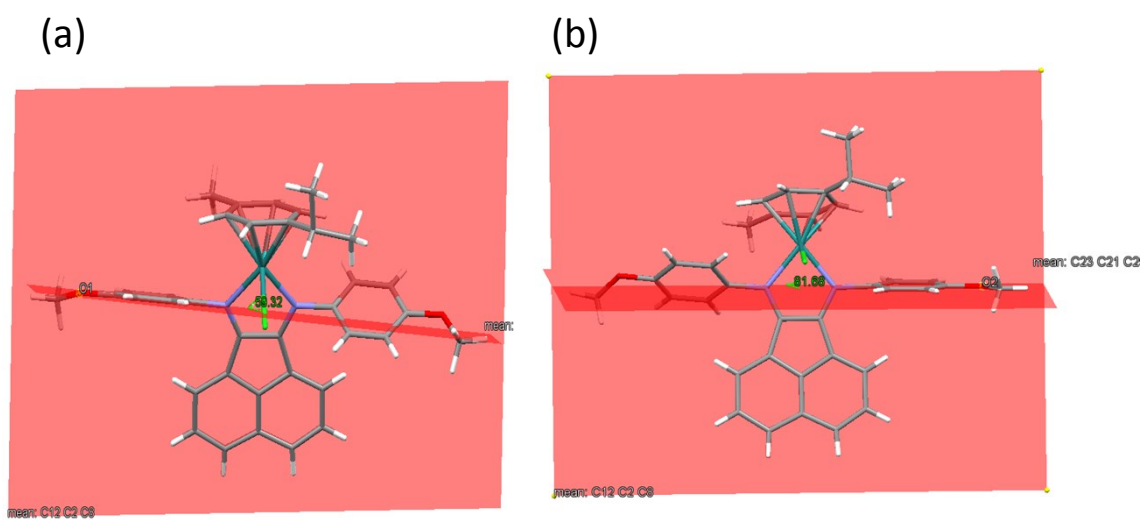


Figure S5. View of dihedral angle between (a) the planes of acenaphthene ring and (O1)-methoxyphenyl ring and (b) the planes of acenaphthene ring and (O2)-methoxyphenyl ring in the structure of Ru(*p*-cym)(NN)(Cl).

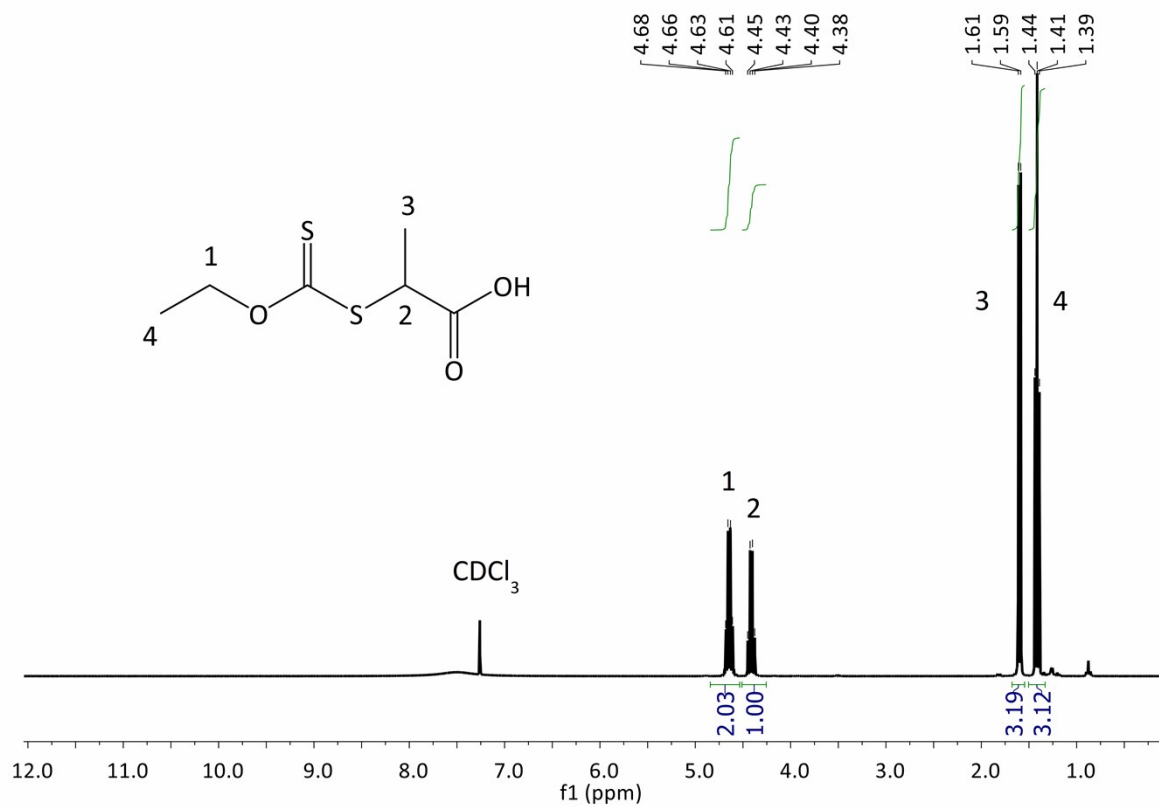


Figure S6. ¹H NMR spectrum of MADIX-COOH measured in CDCl₃.

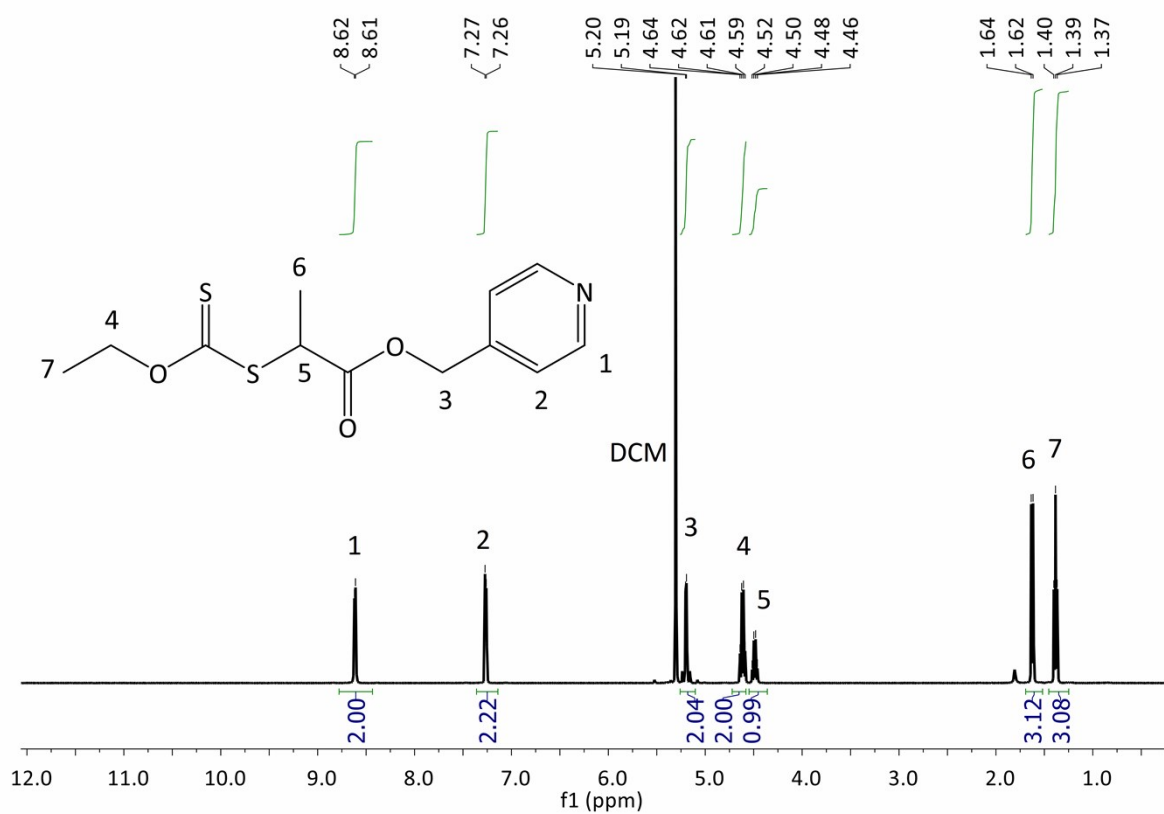


Figure S7. ¹H NMR spectrum of MADIX-Py measured in CDCl₃ (DCM present as impurity)

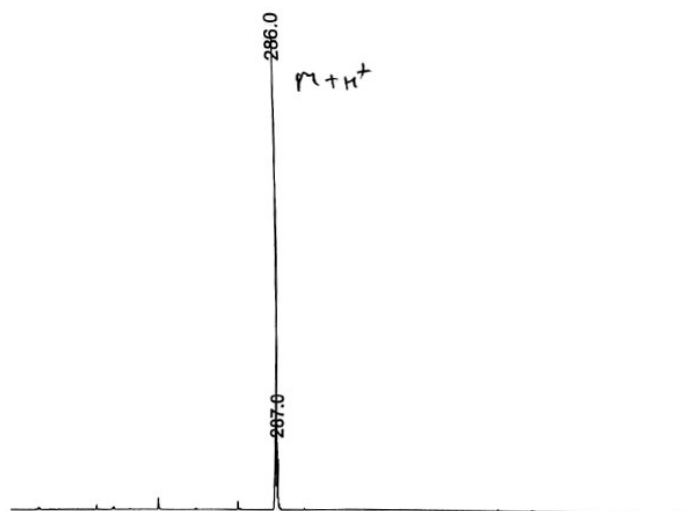


Figure S8. LC-MS of MADIX-Py CTA.

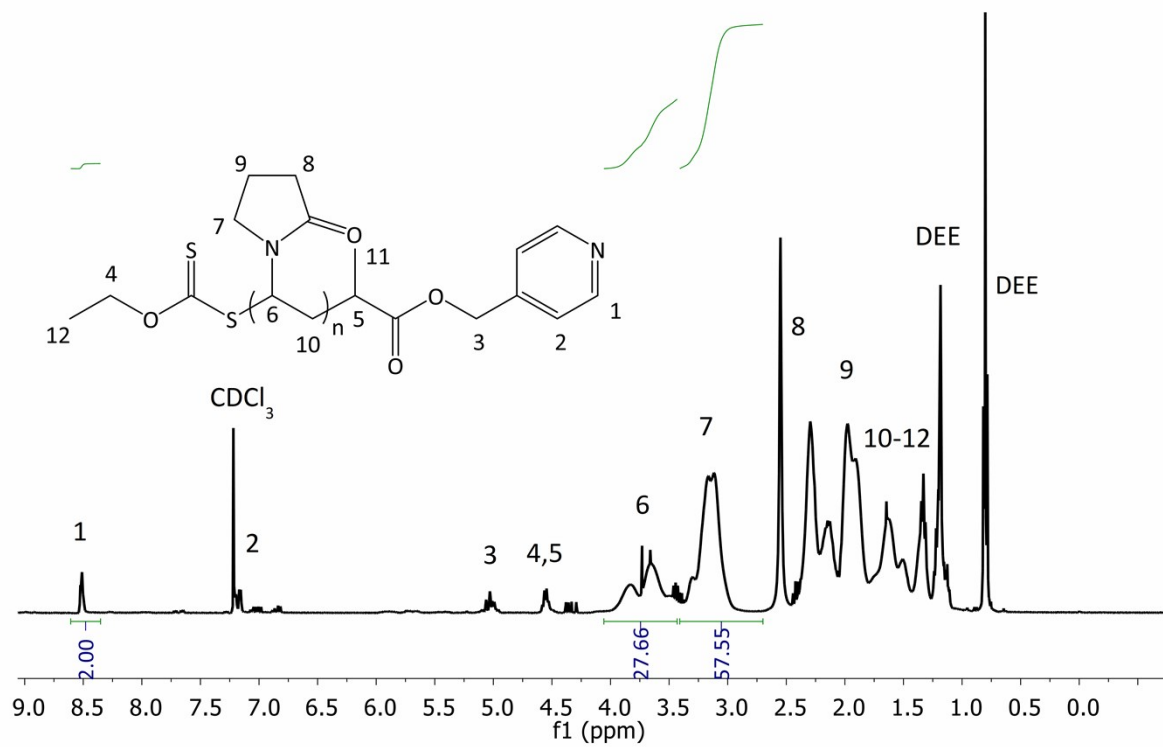


Figure S9. ¹H NMR spectrum of PNVP-Py measured in CDCl₃.

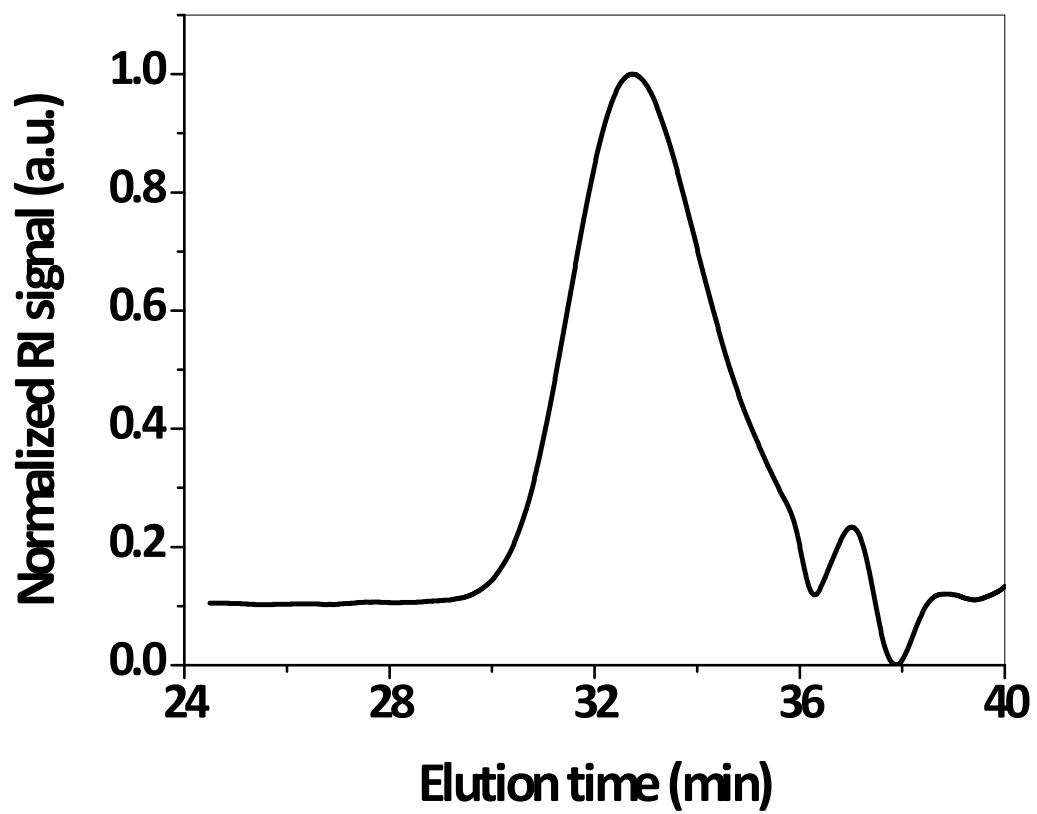


Figure S10. SEC RI traces of PNVP-Py measured in DMAc containing 50 mM of LiCl at 50 °C.

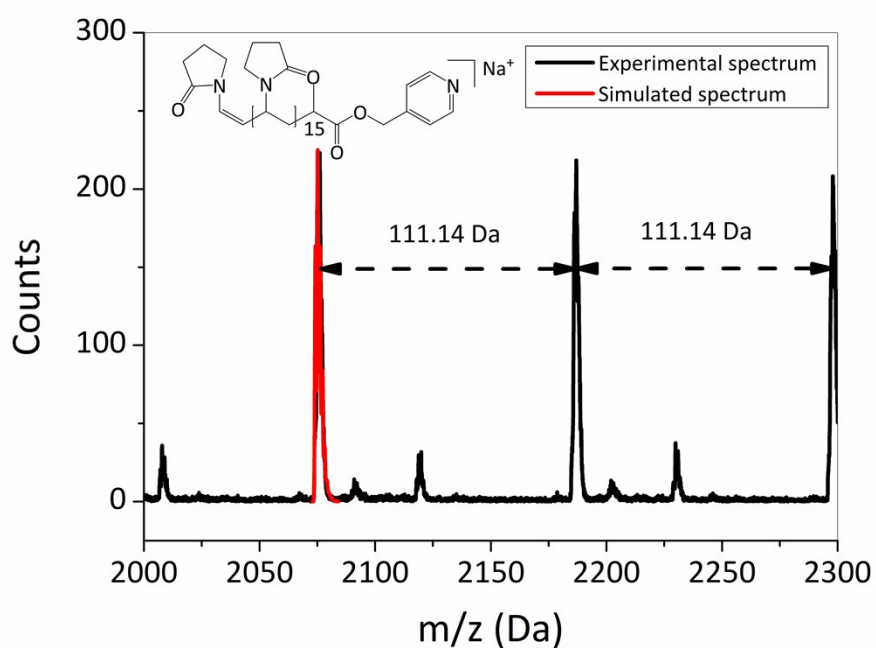
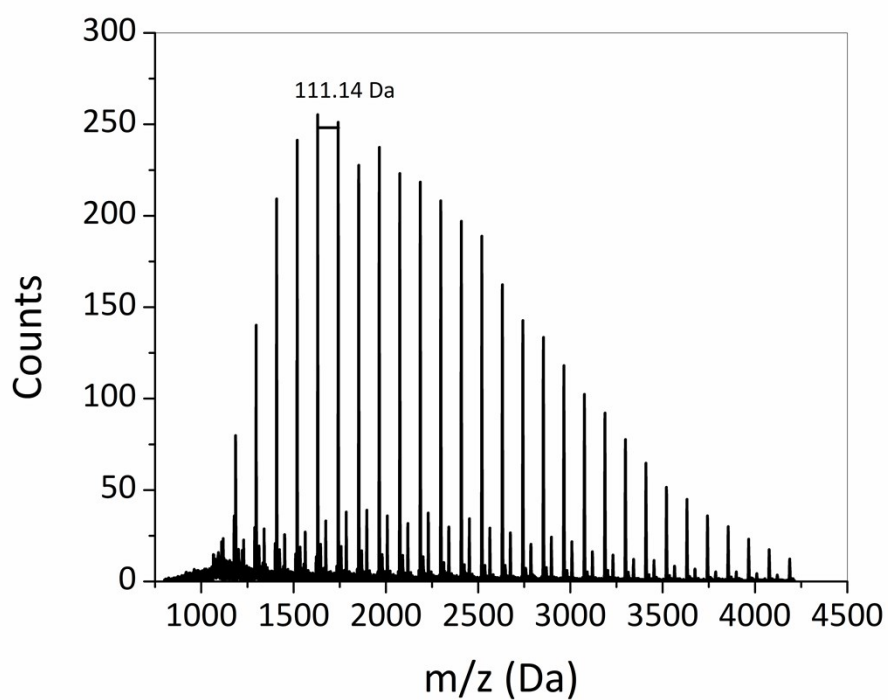


Figure S11. Top) MALDI-TOF mass spectrum of a PNVP-Py synthesized by RAFT/MADIX polymerization in anisole at 60°C for 2.5 h; bottom) Zoom and overlay of experimental spectrum with the simulated spectra of the proposed structure.

Table S3. Structural details of PNVP-Py polymers synthesized via RAFT/MADIX homo polymerization of NVP at 60 °C using anisole as polymerization solvent.

Polymers	[NVP]:[CTA]:[I]	Time (min)	Conv. [%] ^a	DP ^b	M _{n,theo.} [g/mol] ^c	M _{n,NMR} [g/mol] ^d	M _{n,SEC} [g/mol] ^e	Đ ^f
PNVP-Py	[150]:[1]:[0.3]	150	15	23	2800	3400	4200	1.22

^aDetermined by GC with anisole as internal standard; ^bDegree of polymerization (DP) calculated from GC conversion and the used ratio of [NVP]/[CTA]; ^cM_{n,theo.} = ([NVP]/[CTA] x conversion x M_{NVP}) + M_{CTA}; ^dDetermination by end group analysis; ^eDetermined by SEC in DMA containing 50 mM of LiCl at flow rate of 0.500 mL/min using PMMA calibration; ^fĐ = dispersity (M_w/M_n).

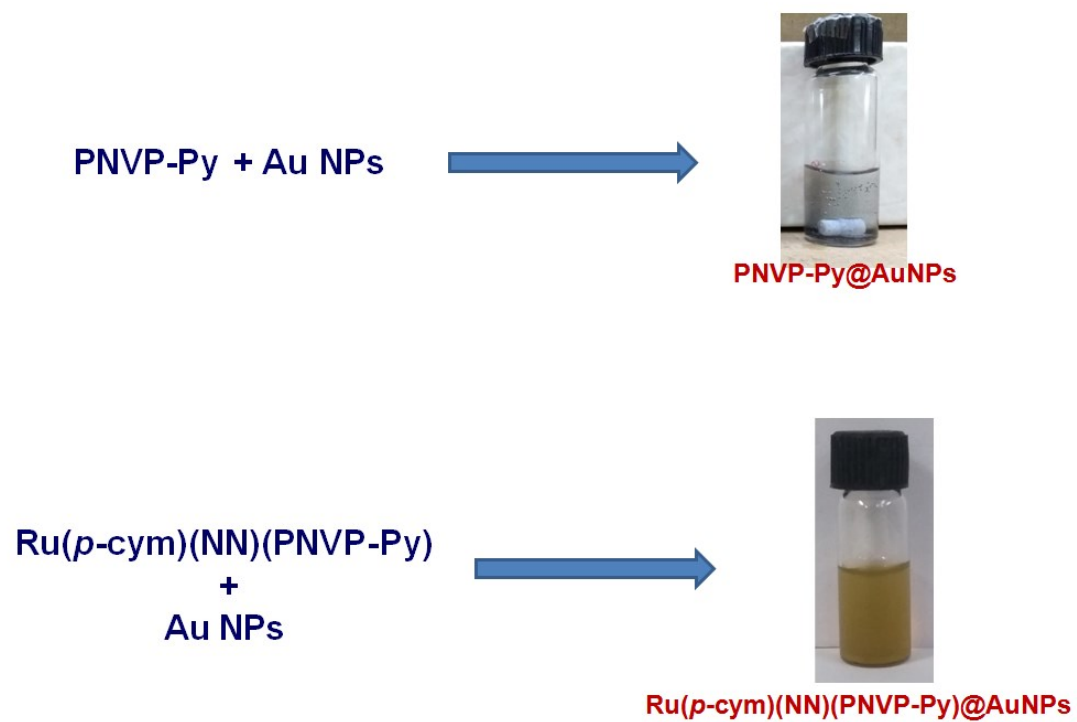
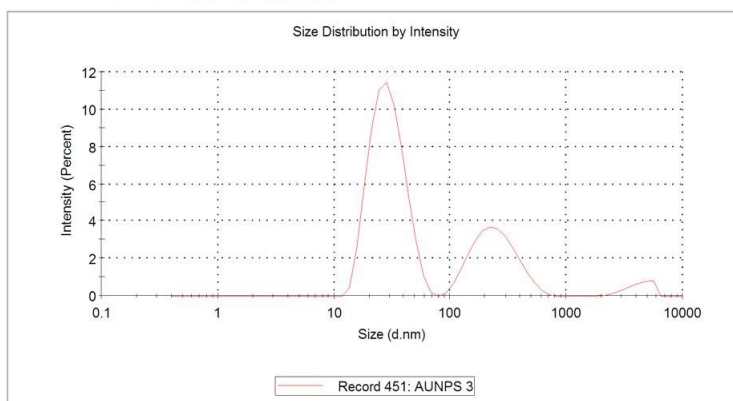


Figure S12. Photographs of glass vials containing PNVP-Py@AuNPs and Ru(*p*-cym)(NN)PNVP-Py@AuNPs in water.

	Size (d.nm):	% Intensity:	St Dev (d.n...)
Z-Average (d.nm): 33.10	Peak 1: 29.79	68.1	9.844
Pdl: 0.630	Peak 2: 255.9	28.4	109.4
Intercept: 0.871	Peak 3: 4288	3.5	973.1

Result quality : Refer to quality report



results

	Size (d.nm):	% Intensity:	St Dev (d.n...)
Z-Average (d.nm): 1012	Peak 1: 164.9	100.0	4.227
Pdl: 1.000	Peak 2: 0.000	0.0	0.000
Intercept: 1.32	Peak 3: 0.000	0.0	0.000

Result quality : Refer to quality report

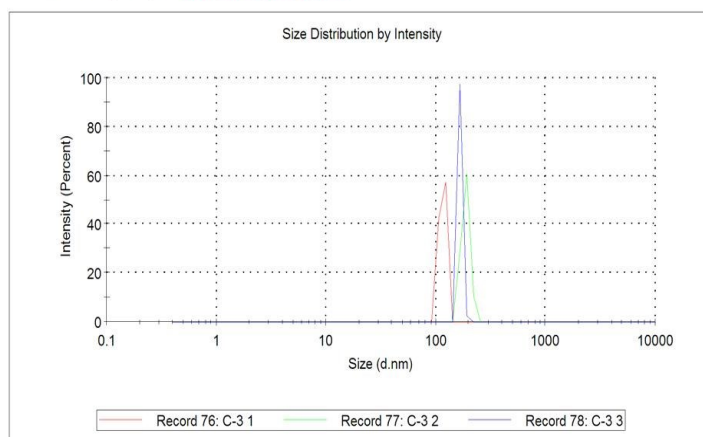


Figure S13. Particle size distribution of AuNPs and Ru(*p*-cym)(NN)(PNVP-Py)@AuNPs measured by DLS analysis. The observation of second and third large particle distributions in the intensity plot of bare AuNPs account to less than one percent of all particles present.

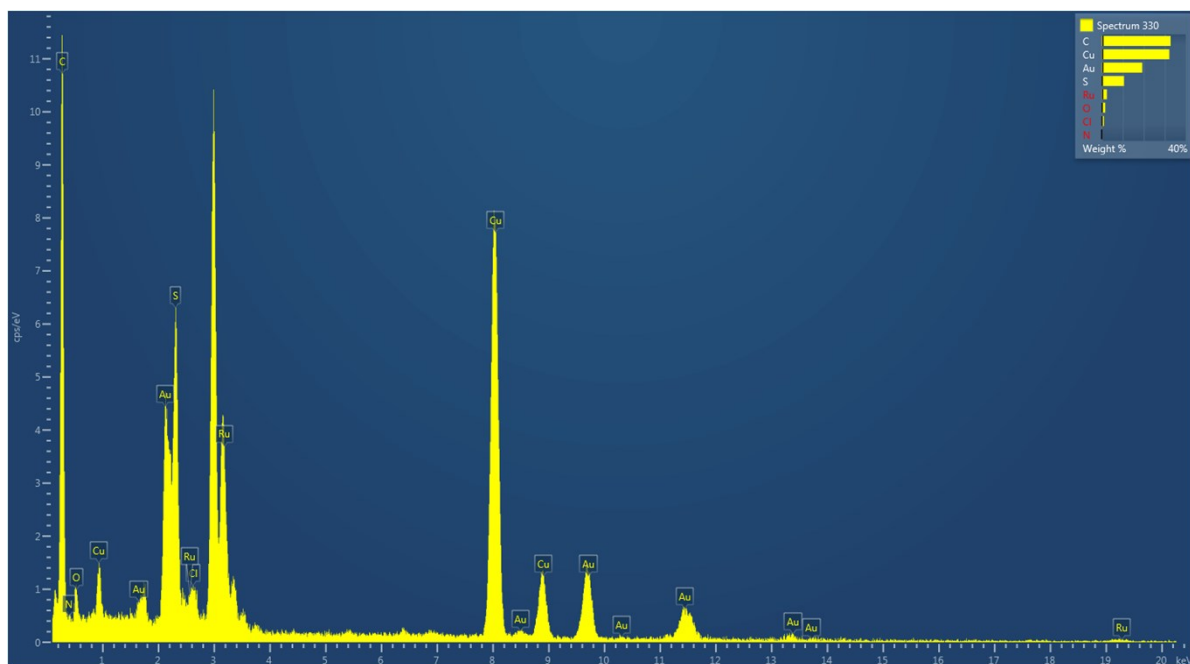
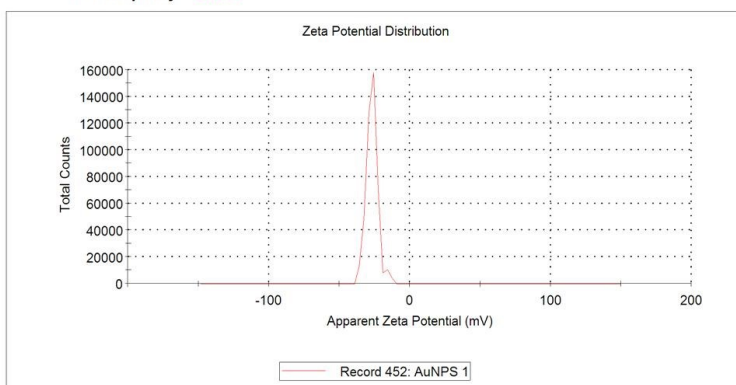


Figure S14. EDX analysis of Ru(*p*-cym)(NN)(PNVP-Py)@AuNPs

	Mean (mV)	Area (%)	St Dev (mV)
Zeta Potential (mV): -26.7	Peak 1: -27.1	94.8	3.48
Zeta Deviation (mV): 4.09	Peak 2: -16.4	5.2	2.37
Conductivity (mS/cm): 1.08	Peak 3: 0.00	0.0	0.00
Result quality : Good			



	Mean (mV)	Area (%)	St Dev (mV)
Zeta Potential (mV): -20.1	Peak 1: -27.4	43.8	4.29
Zeta Deviation (mV): 9.01	Peak 2: -18.0	35.0	3.43
Conductivity (mS/cm): 0.524	Peak 3: -7.67	21.2	3.31
Result quality : Good			

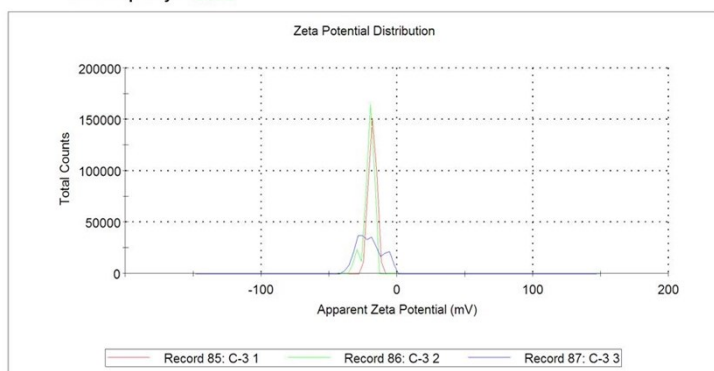


Figure S15. Zeta potential measurement of AuNPs and Ru(*p*-cym)(NN)(PNVP-Py)@AuNPs.

Table S4. Cleavage of supercoiled pBR322 DNA (40 μ M) by Ru(*p*-cym)(NN)(PNVP-Py)@AuNPs and Ru(*p*-cym)(NN)(Cl) in absence of an external agent in 5 mM Tris HCl/50 mM NaCl buffer at 37 °C. Lane 1 : DNA; Lane 2 : DNA + Ru(*p*-cym)(NN)(PNVP-Py)@AuNPs (100 μ M); Lane 3 : DNA + Ru(*p*-cym)(NN)(Cl) (100 μ M).

Lane number	Reaction conditions	Form (%)	
		SC	NC
1	DNA	97.9	2.1
2	DNA+Ru(<i>p</i> -cym)(NN)(PNVP-Py)@AuNPs (100 μ M)	98.5	1.5
3	DNA + Ru(<i>p</i> -cym)(NN)(Cl) (100 μ M)	40.6	59.4

Table S5. Concentration dependent cleavage of pBR322 DNA (40 μM) by Ru(*p*-cym)(NN)(Cl) complex in absence of an external agent in 5 mM Tris HCl/50 mM NaCl buffer at 37 °C. Lane 1 : DNA; Lane 2 : DNA + Ru(*p*-cym)(NN)(PNVP-Py)@AuNPs (100 μM); Lane 3 : DNA + Ru(*p*-cym)(NN)(Cl) (10 μM); Lane 4 : DNA + Ru(*p*-cym)(NN)(Cl) (20 μM); Lane 5: DNA + Ru(*p*-cym)(NN)(Cl) (40 μM); Lane 6 : DNA + Ru(*p*-cym)(NN)(Cl) (60 μM); Lane 7 : DNA + Ru(*p*-cym)(NN)(Cl) (80 μM); Lane 7: DNA + Ru(*p*-cym)(NN)(Cl) (100 μM).

Lane number	Reaction conditions	Form (%)	
		SC	NC
1	DNA	98.5	1.5
2	DNA + Ru(<i>p</i> -cym)(NN)(PNVP-Py)@AuNPs (100 μM)	97.8	2.2
3	DNA + Ru(<i>p</i> -cym)(NN)(Cl) (10 μM)	97.1	2.9
4	DNA + Ru(<i>p</i> -cym)(NN)(Cl) (20 μM)	96.7	3.3
5	DNA + Ru(<i>p</i> -cym)(NN)(Cl) (40 μM)	94.3	5.7
6	DNA + Ru(<i>p</i> -cym)(NN)(Cl) (60 μM)	96.7	3.3
7	DNA + Ru(<i>p</i> -cym)(NN)(Cl) (80 μM)	47.9	52.1
8	DNA + Ru(<i>p</i> -cym)(NN)(Cl) (100 μM)	45.3	54.7

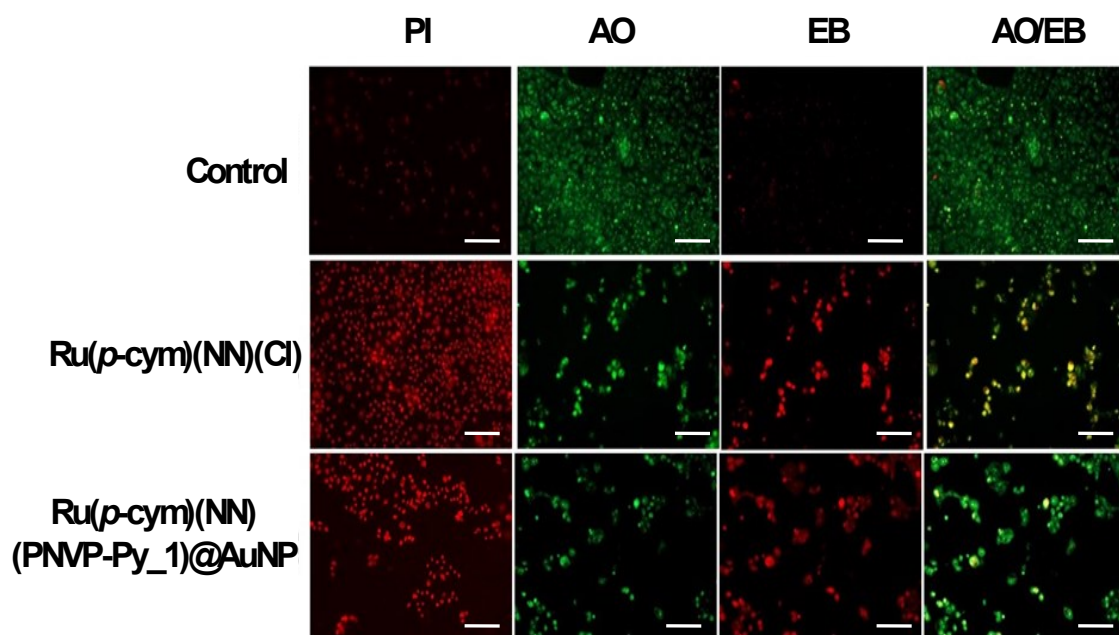


Figure S16. Morphological evidence of apoptosis by PI Staining and AO/EB dual staining. Fluorescent microscopic images of human colorectal adenocarcinoma (HT-29) cell lines after treatment with IC_{50} concentration of Ru(*p*-cym)(NN)(Cl) and Ru(*p*-cym)(NN)(PNVP-Py)₁@AuNPs (Scale bar-100 μ m) .

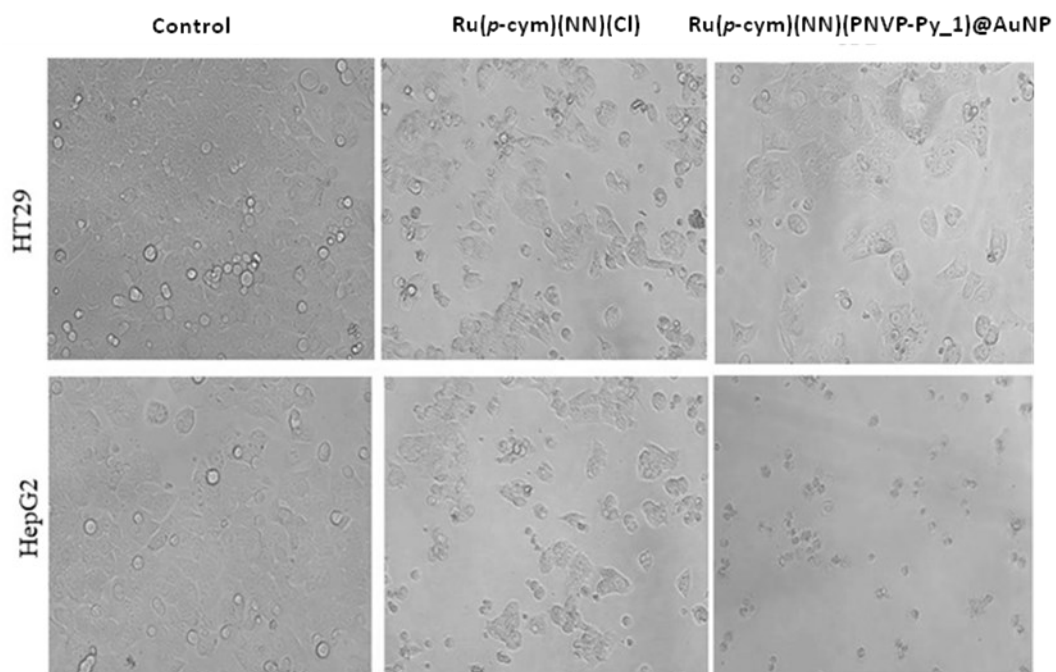


Figure S17. Phase contrast microscopic images of human liver carcinoma (HepG2) and human colorectal adenocarcinoma (HT-29) cell lines after treatment with IC_{50} concentration of $\text{Ru}(p\text{-cym})(\text{NN})(\text{Cl})$ and $\text{Ru}(p\text{-cym})(\text{NN})(\text{PNVP-Py})\text{@AuNPs}$.

REFERENCES

- 1 G. Gomori, Buffers in the Range of pH 6.5 to 9.6. *Proc. Soc. Exp. Biol. Med.*, 1946, **62**, 33.
- 2 M. Gasperini, F. Ragaini, and S. Cenini, Synthesis of Ar-BIAN Ligands (Ar-BIAN=Bis(aryl)acenaphthenequinonediimine) Having Strong Electron-Withdrawing Substituents on the Aryl Rings and Their Relative Coordination Strength toward Palladium(0) and -(II) Complexes. *Organometallics*, 2002, **21**, 2950-2957.
- 3 G. Pound, Z. Eksteen, R. Pfukwa, J.M. Mckenzie, R. F. M. Lange, and B. Klumperman, Unexpected Reactions Associated with the Xanthate-Mediated Polymerization of *N*-Vinylpyrrolidone. *J. Polym. Sci., Part A: Polym. Chem.*, 2008, **46**, 6575–6593.
- 4 N. Vanparijs, S. Maji, B. Louage, L. Voorhaar, D. Laplace, Q. Zhang, Y. Shi, . E. Hennink, R. Hoogenboom, and B.G. De Geest, Polymer-Protein Conjugation Via a ‘Grafting To’ Approach – A Comparative Study of the Performance of Protein-Reactive RAFT Chain Transfer Agents. *Polym. Chem.*, 2015, **6**, 5602-5614.
- 5 S. Maji, Z. Zhang, L. Voorhaar, S. Pieters, B. Stubbe, S. Van Vlierberghe, P. Dubruel, B.G. De Geest, and R. Hoogenboom, Thermoresponsive Polymer Coated Gold Nanoparticles: From MADIX/RAFT Copolymerization of *N*-Vinylpyrrolidone and *N*-Vinylcaprolactam to Salt and Temperature Induced Nanoparticle Aggregation. *RSC Adv.*, 2015, **5**, 42388-42398.
- 6 M. M. Calvo, K. N. Orange, R. B. Elmes, B. la Cour Poulsen, D. C. Williams, and T.Gunnlaugsson, Ru(II)-Polypyridyl Surface Functionalised Gold Nanoparticles as DNA Targeting Supramolecular Structures and Luminescent Cellular Imaging Agents. *Nanoscale*, 2016, **8**, 563-574.
- 7 S. Y. Jeong, S. Y. Park, Y.H. Kim, M. Kim, and S.J. Lee, Cytotoxicity and Apoptosis Induction of Bacillus Vallismortis BIT-33 Metabolites on Colon Cancer Carcinoma Cells. *J. Appl. Microbiol.*, 2008, **104**, 796-807.
- 8 S. N. Nagabhishek, and A. A Madankumar, Novel Apoptosis-Inducing Metabolite Isolated From Marine Sponge Symbiont Monascus Sp. NMK7 Attenuates Cell Proliferation, Migration and ROS Stress-Mediated Apoptosis in Breast Cancer Cells. *RSC Adv.*, 2019, **9**, 5878-5890.
- 9 K. Liu, P.C. Liu, R. Liu, and X. Wu, Dual AO/EB Staining to Detect Apoptosis in Osteosarcoma Cells Compared with Flow Cytometry. *Med. Sci. Monit. Basic Res.*, 2015, **21**, 15-20.